NASA TM-86918

1985000 7990

DOE/NASA/20320–61
NASA TM–86918

NASA-TM-86918

Shutdown Characteristics of the Mod-0 Wind Turbine with Aileron Controls

Dean R Miller and Robert D Corrigan
National Aeronautics and Space Administration
Lewis Research Center

NF00112

DISCLAIMER

This report was prepared as an account of work sponsored by an agency of the United States Government Neither the United States Government nor any agency thereof, nor any of their employees, makes any warranty, express or implied, or assumes any legal liability or responsibility for the accuracy, completeness, or usefulness of any information, apparatus, product, or process disclosed, or represents that its use would not infringe privately owned rights Reference herein to any specific commercial product, process, or service by trade name, trademark, manufacturer, or otherwise, does not necessarily constitute or imply its endorsement, recommendation, or favoring by the United States Government or any agency thereof The views and opinions of authors expressed herein do not necessarily state or reflect those of the United States Government or any agency thereof

Shutdown Characteristics of the Mod-0 Wind Turbine with Aileron Controls

Dean R Miller and Robert D. Corrigan
National Aeronautics and Space Administration
Lewis Research Center
Cleveland, Ohio 44135

N85-16299

SHUTDOWN CHARACTERISTICS OF THE MOD-0 WIND TURBINE WITH AILERON CONTROLS

Dean R. Miller and Robert D. Corrigan
National Aeronautics and Space Administration
Lewis Research Center
Cleveland, Ohio 44135

SUMMARY

Horizontal-axis wind turbines utilize partial or full variable blade pitch to regulate rotor speed. The weight and costs of these systems indicated a need for alternate methods of rotor control. Aileron control is an alternative which has potential to meet this need.

The NASA Lewis Research Center has been experimentally testing aileron control rotors on the Mod-0 wind turbine to determine their power regulation and shutdown characteristics.

This paper presents experimental and analytical shutdown test results for a 38 percent chord aileron-control rotor. These results indicated that the 38 percent chord ailerons provided overspeed protection over the entire Mod-0 operational windspeed range, and had a no-load equilibrium tip speed ratio of 1.9. Thus, the 38 percent chord ailerons had much improved aerodynamic braking capability when compared with the first aileron-control rotor having 20 percent chord ailerons.

INTRODUCTION

As part of the DOE Wind Energy Program, the NASA Lewis Research Center (LeRC) has been involved in the research of large horizontal-axis wind turbines since 1973. The overall goal of the effort has been to develop the technology to build reliable, yet cost effective large HAWTS. Since the rotor constitutes a large portion of the overall wind turbine cost, various methods of rotor control were investigated based on their potential to reduce rotor weight and cost.

Aileron control was a method of rotor control which appeared to have potential for reducing rotor costs. This method of rotor control involved placing a control surface on the trailing-edge of the rotor blade (in the same way control surfaces are placed on the trailing edges of aircraft wings). As with the airplane wing, the ailerons change the lift and drag characteristics of the basic airfoil as a function of their deflection angle, producing corresponding changes in rotor torque. It is these changes in rotor torque which enable the ailerons to regulate rotor speed or rotor power output.

The primary advantages of aileron control over partial-span control are that a smaller pitch actuator system is required and the actuator system can be located so as not to interrupt the structure of the blade spar. The net result is a lighter weight, less complicated actuator system than that used for partial-span control.

To investigate the applicability of aileron control to large horizontal-axis wind turbines a feasibility study was performed by Wichita State

University (ref. 1). Based on this study, two outboard blade tip sections with 20 percent chord ailerons were designed and fabricated for testing on the Mod-0 100 kW wind turbine. These tips were installed on existing inboard blades to form an aileron-control rotor. Loss-of-load shutdown tests and no-load equilibrium rpm tests were conducted and the results indicated that the 20 percent chord ailerons did not provide enough aerodynamic braking capability.

Therefore, two blade tip sections were designed with 38 percent chord ailerons and fabricated for testing on the Mod-0. These 38 percent chord aileron-control tips were also installed and tested on the Mod-0. Test results with this rotor showed much improved aerodynamic braking characteristics, when compared to the 20 percent chord aileron-control rotor.

This paper will describe the Mod-0 test facility and explain the two types of shutdown tests conducted on the Mod-0 with the 38 percent chord ailerons: (1) overspeed, (2) no-load equilibrium rotor speed. Then, experimental overspeed test results will be compared with analytical predictions for windspeeds up to 12 m/s. Since no experimental overspeed data were available for winds above 13 m/s, the analytical overspeed predictions will then be extended to cover the windspeed range of 13 to 18 m/s (where 18 m/s = Mod-0 cutout windspeed). Next, experimental equilibrium rpm test results will be presented and compared with analytical predictions, followed by a summary of both the overspeed and equilibrium rpm test results.

TEST CONFIGURATION

Shutdown tests were conducted on the Mod-0 100 kW wind turbine located at Plumbrook Station, Sandusky, Ohio. Figure 1 shows the the configuration of the Mod-0 which operated downwind of the tower with a teetered hub. The nacelle was located atop a tubular tower with the rotor axis 38 m above the ground.

The planform of the rotor used in these tests is shown in figure 2. The inboard portion of each rotor blade consisted of two pieces - a metal spool piece and an 11.2 m wood blade. The metal spool piece served as an adapter between the steel teetered-hub and the wooden blade. The wooden blade was untwisted, fixed at a pitch angle of 0°, and used a NACA 23024 airfoil section over the entire length.

The outboard section of each blade was 7.28 m long and contained an aileron section 6.09 m long. It was a riveted aluminum structure, fabricated using standard aircraft technology. The aileron was hinged at the 62 percent chord line and extended over the outer 32 percent of the blade span (neglecting the tip cap). The portion of the tip between spanwise station (STA) 12.22 and 13.09 was considered to be a transition section between the inboard wooden blade with its NACA 23024 airfoil section and the beginning of the aileron with its NACA 64624 airfoil. This transition section not only provided for a change in airfoil section, but also for a change in twist angle (linearly varying from 0° twist at STA 12.22 to 3° at STA 13.09). The thickness of the tip section decreases linearly from 24 percent at STA 13.11 to 15 percent at STA 19.20. Also, the twist angle varies from 3° at STA 13.11 to 1° at STA 19.20. Figure 3 shows the twist angle distribution and sign convention for the aileron-control tip.

2

Figure 4 is a planform arrangement of the blade tip section with a cross-sectional view of the 38 percent chord plain aileron. Also, indicated is the sign convention for the aileron deflection. A negative deflection corresponds to rotating the trailing edge of the aileron away from the wind (i.e., - towards the low pressure surface of the blade). During shutdown tests the ailerons were deflected in the negative direction to produce a braking effect.

TEST DESCRIPTION

The aerodynamic braking tests conducted on the 20 percent and 38 percent chord aileron-control rotors were (1) rotor overspeed following loss of load, and (2) no-load equilibrium rotor speed. The relationship between these two tests is illustrated in figure 5, which is a rotor speed time history for a hypothetical loss-of-load shutdown.

The shutdown has been divided into a rotor overspeed test and a no-load equilibrium rpm test. The rotor overspeed test defines the time period immediately following a loss of generator load. It is during this time period after the load is removed and before the ailerons are completely deflected that the rotor may experience large accelerations, thus producing an overspeed and possible damage to the drive train and generator. Therefore, it is important for the aileron-control system to either prevent an overspeed or limit the peak rpm to a safe value.

The no-load equilibrium test is characterized by the rotor reaching a stable or equilibrium rpm which is a function of the windspeed. This can be seen in figure 5 as the portion of the rotor speed time history where the curve parallels the abscissa. Should the windspeed change, the rotor speed would also change to a new equilibrium rotor speed.

LOSS-OF-LOAD OVERSPEED TEST

Test Procedure

The Mod-0 was aligned with the wind and producing power before the generator load was disconnected. Both ailerons were fixed at a deflection angle of 0°; thus the output power varied as a function of windspeed. When the windspeed appeared to be relatively constant, the generator load was dropped, and one or both ailerons were moved toward the shutdown position of -90°. Though it was intended for the loss of load and aileron deflection to occur simultaneously, the ailerons actually began to move toward shutdown 1 sec after the loss of load occurred. This was attributed to mechanical and electrical delays in the aileron-control system.

Loss-of-load shutdowns were performed with the ailerons of both blades deflecting (2-aileron shutdown), or with the aileron of only one blade deflecting with the other aileron fixed at 0° deflection (1-aileron shutdown). For both the 1- and 2-aileron shutdowns, fixed deflections rates of 15, 20, and 25 deg/sec were used.

3

Experimental Data Analysis

Experimental loss of load tests were conducted with both ailerons initially at 0° deflection. This represented a "worse case" situation, because in the power regulation mode, the ailerons would probably have a negative initial deflection angle at windspeeds above 8 m/s, where rated power is achieved.

Windspeed and rotor speed were recorded at 1 sec intervals during each of the overspeed shutdowns using an HP-85 computer. Experimental rotor speed time histories were then constructed by plotting rotor speed versus the elapsed time. These experimental time histories were then compared with analytical time histories on the basis of peak overspeed and general shape of the deceleration curve.

Predicted Data Analysis

The Mod-0 Emergency Shutdown Model (ref. 2) was used to predict the rotor speed time history following loss of generator load. Probably the most critical part of the analytical prediction involved the selection of airfoil lift and drag coefficients which were used in the Shutdown Model to calculate rotor torque. The appropriate airfoil characteristics had to be selected for the inboard wood blade with its untwisted NACA 23024 airfoil, as well as for the aileron-control tip with its twisted NACA 64 series airfoil.

Since the aerodynamic characteristics of the aileron-control tip varied with the aileron deflection angle, it was necessary to have a separate table of lift and drag data for each aileron deflection studied. This meant that airfoil data were required for -45°, -60°, -75°, and -90° aileron deflection angles. Some two-dimensional data were available from the Ohio State University wind tunnel, but only up to 35° angle of attack. Because the range of angle of attack values on the tip was expected to exceed 35°, it then was necessary to estimate lift and drag data out to 90° angle of attack based on Wichita State University 20 percent chord aileron data. The preliminary equilibrium rotor speed predictions based on these data showed poor agreement with preliminary experimental results.

It was then decided to utilize three-dimensional data (midspan Reynolds number = 1.5×10^6) from the full-scale tests of an identical 38 percent chord aileron blade tip which was tested in NASA Langley's 30 ft by 60 ft Wind Tunnel (figs. 6(a) and (b)). These full-scale test data were selected for several reasons:

(1) The three-dimensional full-scale test data when compared with existing two-dimensional data showed similar trends. The agreement between the available two-dimensional data and corresponding three-dimensional data was very close for an aileron deflection of -90°.

(2) These three-dimensional data were available at aileron deflection angles of -40°, -60°, -75°, and -90° from 0° to 90° angle of attack; hence the post-stall characteristics were clearly defined beyond 35° angle of attack.

(3) Three-dimensional flow effects near the tip were inherent in the three-dimensional full scale tests, therefore, no tip loss would be required in the Shutdown Model.

4

(4) The actual geometry of the 38 percent chord aileron-control tip was complex. It had a varying twist, combined with changes in thickness to chord ratio. In addition, the airfoil cross section changed from a NACA 23024 to a NACA 64 series airfoil inboard of the aileron section. As such, it was thought that proper treatment of these geometry changes would require a significant amount of additional time to complete. Since the full-scale test data represented an integrated average of these effects, it was decided to use these three-dimensional data which eliminated the need to make corrections for the variations in geometry.

For the wooden inboard portion of the rotor, WSU 23024 test results (Re = 0.6×10^6) were used with post-stall data synthesized according to the procedure set forth in reference 3. The post stall lift and drag data were synthesized to yield a constant torque after stall, but no aspect ratio correction was employed. This was done to account for the apparent tendency of the inboard blade sections to produce positive torque for angles of attack beyond the two-dimensional stall angle. Both the synthesized and unsynthesized 23024 data are shown for comparison purposes in figures 6(c) and (d).

Discussion of Results

For each of the overspeed shutdowns, the analytical and experimental time histories were compared. Figures 7(a) and (b) show typical rotor speed time histories for a 1- and 2-aileron shutdown, respectively. These curves illustrate that the analytical predictions agreed quite well with the experimental results.

Figure 8 is a plot of peak rotor speed versus windspeed for 2-aileron shutdowns at various deflection rates. The operational rotor speed, prior to loss-of-load, was nominally 20 rpm for these shutdowns. The symbols (circle, square, and triangle) represent experimental peak rotor speeds for deflection rates of 15, 20, and 25 deg/sec, respectively. These peak rotor speeds were plotted against the average windspeed which occurred during the first 6 sec of the experimental shutdown.

The curves (dashed, solid, and dot-dashed) represent the predicted peak rotor speeds for deflection rates of 15, 20, and 25 deg/sec, respectively. These curves pass through the bulk of the data, thus indicating good agreement between the experimental and analytical peak rotor speeds. The differences between the experimental data and the analytical predictions can be, in part, attributed to the fact that the predictions are based on constant wind conditions where as during the actual shutdown, neither the windspeed nor wind direction remained constant.

To quantify this variation in experimental peak rotor speeds, the "percent discrepancy" between experimental and analytical peak rotor speeds was calculated for each shutdown. The expression shown below was used to calculate this parameter:

$$\text{Percent discrepancy} = \frac{\text{Peak rpm (Exp)} - \text{Peak rpm (Pred)}}{\text{Peak rpm (Pred)}} \times 100$$

These discrepancy values were used to construct a histogram, from which an "error band" was then determined. This error band was intended to identify

the accuracy of the predictions by accounting for unsteady experimental conditions.

Figure 9 is a histogram of the discrepancy between predicted and experimental 2-aileron peak rotor speeds. The plot appears to have a normal distribution with most of the discrepancies between +4 and -4 percent. Based on this, it seemed reasonable to place an error band of ±4 percent on 2-aileron peak rotor speed predictions. For example, if the predicted peak rotor speed were 25 rpm, then the experimental rotor speed would range from 24 to 26 rpm.

With the discrepancy between analytical and predicted results established, the next step was to extend the predictions to higher windspeeds as shown in figure 8. Deploying both ailerons at a rate of 25 deg/sec in a windspeed of 18 m/s resulted in a predicted peak rotor speed of 24.3 rpm. If the ±4 percent error band were to be considered, the peak rotor speed could be expected to range from 23.3 to 25.2 rpm. For an initial rotor speed of 20.5 rpm, this would correspond to a peak overspeed ranging from 14 to 23 percent. Thus, should a loss-of-load occur at the cutout windspeed, the 38 percent chord aileron-control rotor should limit the peak rotor overspeed to 23 percent above the nominal rotor speed of 20 rpm (assuming 2-ailerons deflecting at 25 deg/sec).

The analytical results in figure 8 also suggest that increasing the deflection rate should decrease the peak rotor speed. For example, increasing the deflection rate from 15 to 25 deg/sec should lower the peak rotor speed by 2 rpm in an 18 m/s wind. Thus, the aileron deflection rate has a significant effect on the peak rotor overspeed.

Figure 10 is a plot of peak rotor speed versus windspeed for 1-aileron shutdowns at various deflection rates. The operational rotor speed, prior to loss-of-load, was nominally 20 rpm for these shutdowns. The symbols (circle, square, and triangle) represent experimental peak rotor speeds for deflection rates of 15, 20, and 25 deg/sec, respectively. These peak rotor speeds were plotted against the average windspeed which occurred in the first 6 sec of the experimental shutdown.

The curves (dashed, solid, and dot-dashed) represent the predicted peak rotor speeds for deflection rates of 15, 20, and 25 deg/sec, respectively.

The experimental data shown in figure 10 exhibited more deviation from the predicted curves, than did the 2-aileron shutdown data in figure 8. This may be partially due to the larger teeter motions which occur during the 1-aileron shutdowns.

Figure 11 is a histogram of the discrepancy between predicted and experimental 1-aileron peak rotor speeds. Here the distribution is skewed, such that the analytical model over predicts peak rotor speeds with the discrepancies between -8 and +4 percent. As with the 2-aileron shutdowns, this range of discrepancies (-8 to +4 percent) was treated as an error band to be used in conjunction with the predicted values. The lower limit of -8 percent suggests that the analytical model tended to overpredict the peak rotor speed.

The predicted peak rotor speed for a deflection rate of 25 deg/sec and a windspeed of 18 m/s is 25.8 rpm. Considering the -8 to +4 percent error band, this would translate to a peak rotor speed ranging in value from 23.8 to

6

26.8 rpm. For an initial rotor speed of 20.5 rpm, this would correspond to a peak overspeed ranging from 16 to 31 percent. Thus, should a loss-of-load occur at the cutout windspeed, the 38 percent chord aileron-control rotor should limit the peak overspeed to 31 percent above the nominal rotor speed of 20 rpm (assuming 1-aileron deflecting at 25 deg/sec).

This figure again indicates that the larger deflection rates should produce a smaller peak overspeed. It also shows that for similar conditions the peak rotor speed for a 1-aileron shutdown will be higher, than for a 2-aileron shutdown. Consider, for example, the predicted peak overspeed for a loss of load shutdown with a deflection rate of 25 deg/sec and a windspeed of 18 m/s. The peak overspeed should be limited to 23 percent for a 2-aileron shutdown, and 31 percent for a 1-aileron shutdown.

Figure 12 summarizes the effect of deflection rate on the predicted peak rotor speed for 1- and 2-aileron shutdowns. The solid curves represent 2-aileron predictions, while the dashed curves represent 1-aileron predictions. These predictions are shown for windspeeds of 5, 10, and 18 m/s.

This figure illustrates the reduction in peak rotor speed with increased deflection rate. For deflection rates greater than 25 deg/sec and windspeeds above 5 m/s, the curves tend to asymptotically approach a peak rotor speed which is independent of deflection rate and primarily a function of windspeed. However, for a windspeed of 5 m/s, changes in deflection rate have a negligible effect on the peak rotor speed. Thus, the peak rotor speed appears to be a function of not only the deflection rate, but of the windspeed, too.

Another parameter evaluated from the 1- and 2-aileron overspeed tests was the rotor deceleration just after the peak rpm. In this region, the aileron(s) will have already reached the maximum shutdown deflection of -90°. Referring back to figure 5, the deceleration appears to be relatively constant up until 10 sec after the peak rpm. This is indicated by the rpm curve resembling a straight line and thus having a constant rate of change of rpm. Assuming that the deceleration was constant over this time interval, the slope of the rpm curve was then determined from each of the experimental 1- and 2-aileron shutdown time histories for the 10 sec time interval just after peak rpm. These "slopes" (decelerations) were plotted versus the windspeed (at loss-of-load) in figure 13. The data indicate that during this portion of the shutdown, the deceleration was independent of the windspeed and approximately constant at 0.6 rpm/sec for the 1-aileron shutdowns, and 1.2 rpm/sec for the 2-aileron shutdowns.

EQUILIBRIUM ROTOR SPEED TEST

Test Procedure

With the rotor brake applied, the Mod-0 was aligned with the wind. Next both aileron control surfaces were fixed at one of the following deflection angles: -45°, -60°, -75°, or -90°. The rotor brake was then released and a hydraulic motor was used to accelerate the wind turbine to 8 rpm. At this point the motoring was stopped and the rotor was allowed to "freewheel" as a function of windspeed.

Experimental Data Analysis

Rotor speed, aileron deflection angle, and windspeed were recorded on digital tape once per revolution and grouped together to construct 2.5 min averages. Average values of rotor speed were plotted versus average values of windspeed, and these data were fitted with a second order curve fit. These curve fit expressions were subsequently used to derive expressions for equilibrium tip speed ratio as a function of only windspeed. This procedure is illustrated below:

Step 1   Curve fit the data to get a relationship between rpm and V_W:

$$rpm_{EQ} = fo(V_W) \tag{1}$$

Step 2   Definition of tip speed ratio:

$$\lambda_{EQ} = (rpm_{EQ} * 0.1047 * R)/V_W \tag{2}$$

Step 3   Let R = 19.5 m, then Equation (2) becomes:

$$\lambda_{EQ} = 2.041 * (rpm_{EQ}/V_W) \tag{3}$$

Step 4   Replace rpm_{EQ} with $fo(V_W)$:

$$\lambda_{EQ} = 2.041(fo(V_W)/V_W) \tag{4}$$

where

V_W windspeed, m/s

rpm_{EQ} equilibrium rotor speed, rpm

$fo(V_W)$ curve fit equation of equilibrium rotor speed and windspeed

λEQ equilibrium tip speed ratio

R   blade radius

(0.1047)   conversion factor from rpm to rads/sec

Since the equilibrium rpm curve fit equation $fo(V_W)$ is a function of windspeed, the expression for equilibrium tip speed ratio can be expressed solely as a function of windspeed, $\lambda_{EQ} = f_1(V_W)$.

Predicted Data Analysis

The Emergency Shutdown Model was used to predict the equilibrium rotor speed for windspeeds of 5, 10, 15, and 20 m/s, and for deflection angles of -45°, -60°, -75° and -90°. With this matrix of windspeed and aileron deflections, no-load equilibrium rpm was predicted for the ailerons of both blades deflected (2 aileron case), and for the aileron of only one blade deflected with the other aileron fixed at 0° deflection (1 aileron case).

Though the Emergency Shutdown Model was developed to predict peak rotor speed following a loss of generator load, it had the capability to predict no-load equilibrium rotor speed, too. This capability was utilized by simply allowing the computer program to simulate a loss-of-load shutdown and continue calculating rotor speed as a function of time, until the rotor speed no longer changed. This rotor speed represented the predicted equilibrium rpm for a given windspeed and aileron deflection angle.

Discussion of Results

Results of the no-load equilibrium rotor speed tests, with both ailerons deployed (are shown in) figures 14(a) to (d). No-load equilibrium rotor speed is plotted versus windspeed. The experimental data (circles) represent 2.5 min averages, where the wind turbine was within ±10° of direct alignment with the wind, and the generator was electrically disconnected from the utility grid. The solid line fitted through the experimental data was determined by using a second-order least squares regression. The dashed line represents a linear first order curve fit of the equilibrium rpm predicted by the Emergency Shutdown Model. The equations for both the measured and predicted curve fits are shown below the plot. The only difference between figures 14(a) to (d) is the aileron deflection angle. The deflection angles for figures 14(a) to (d) are -45°, -60°, -75°, and -90°, respectively.

Figures 14(a) to (d) show that the slopes of the measured and predicted curves decreased with larger negative aileron deflection angles. This decrease was expected, because experimental lift and drag coefficients for the 38 percent chord aileron suggested a greater "aerodynamic braking capability" at -90° deflection, than at -45° deflection. Also, the measured data exhibited a slight curvature, which required a second order (parabolic) curve to fit the experimental data more accurately.

The overall quality of the experimental data was very good considering the variability in wind speed, wind direction, dynamic effects due to teetering, and wind shear, etc. However, there were some data points with large deviations from the experimental curve fit. These points occurred near 4 rpm for various windspeeds less than 10 m/s, and suggest that the inertia of the rotor may be affecting these results. This is a reasonable explanation because at very low tip speed ratios and large negative aileron deflections, very little positive rotor torque is being produced. In addition, the drive train frictional losses constitute a large percentage of that rotor torque. Hence, the net torque available to accelerate the rotor may be very small, thus making the rotor appear insensitive to small changes in windspeed.

Additional no-load equilibrium rotor speed tests were attempted on the Mod-0 with one aileron deflected at -45°, -60°, -75° or -90°, while the other aileron was fixed at 0°. This simulated 1-aileron jamming in the "full-power" position. Unfortunately the data recorded from these tests were extremely poor, and there was excessive teeter motion which damaged the rubber-teeter stops. As a result, these tests were discontinued and no measured data will be presented for the 1-aileron no-load equilibrium rpm case. However, the Emergency Shutdown Model was used to predict the equilibrium rotor speed for this condition. These results are shown in figure 15, where the equilibrium rotor speed is plotted versus windspeed. There are four curves, one for each deflection angle of the deployed aileron -45°, -60°, -75°, and -90°. These

9

predictions indicate that larger negative aileron deflections will produce smaller equilibrium rotor speeds. This agrees with the measured and predicted results shown in figure 14, for the case where the ailerons of both blades were deployed.

Table I lists equilibrium tip speed ratio equations for the -45°, -60°, -75°, and -90° deflections of the 38 percent chord aileron-control rotor, and shows the computation of rpm_{EQ} and λ_{EQ} for windspeeds of 10, 15, and 20 m/s.

Equilibrium tip speed ratios for the case where only 1 aileron was deployed, and for the case where both ailerons were deployed are compared in figure 16. The curves presented in figure 16 were extracted from figures 14 and 15 for each of the four aileron deflection angles. As expected, the equilibrium tip speed ratios with 1-aileron deployed are higher than the equilibrium tip speed ratios for both ailerons deployed.

SUMMARY OF RESULTS

1. Predicted peak rotor speeds showed close agreement with experimental peak rotor speeds for 1- and 2-aileron shutdowns. Discrepancies of -4 to +4 percent were noted for the 2-aileron shutdowns, while discrepancies of -8 to +4 percent were noted for the 1-aileron shutdowns.

2. The overspeed protection capability of the 38 percent chord ailerons was evaluated for 1- and 2-aileron shutdowns at the cutout windspeed of 18 m/s and a deflection rate of 25 deg/sec. The peak overspeed should be limited to 31 percent with 1 aileron deployed, and 23 percent with 2 ailerons deployed.

3. The rotor slowdown rate, just after peak rpm, was determined from experimental rotor speed time histories of 1- and 2-aileron shutdowns. A comparison of these decelerations indicated that the 2-aileron shutdowns had a deceleration of 1.2 rpm/sec, which was twice that of the 1-aileron shutdowns (0.6 rpm/sec.)

4. The no-load equilibrium tip speed ratios for the 38 percent chord aileron-control rotor are shown below for various aileron deflections (both ailerons deployed):

Deflection, deg	Equilibrium tip speed ratio, λeg
-45	3.4
-60	2.5
-75	2.1
-90	1.9

CONCLUSIONS

1. The agreement between analytical and predicted rotor speed time histories for 1- and 2-aileron shutdowns was very good.

2. The 38 percent chord ailerons provided rotor overspeed protection over the entire Mod-0 operational windspeed range of 4 to 18 m/s.

3. Aileron-control appears to be a viable method for limiting rotor overspeed following a loss of generator load.

REFERENCES

1. Wentz, William H. Jr., Snyder, Melvin H. and Calhoun, John T.: Feasibility Study of Aileron and Spoiler Control Systems for Large Horizontal Axis Wind Turbines, NASA CR-159856, May 1980.

2. Miller, D.R. and Ensworth, C.B.: Analytical Model for Predicting Emergency Shutdown of a Two-Bladed Horizontal-Axis Wind Turbine, NASA TM-83472, June 1983.

3. Viterna, L.A. and Janetzke, D.C.: Theoretical and Experimental Power from Large Horizontal-Axis Wind Turbines, NASA TM-82944, September 1982.

4. Miller, D.R. and Puthoff, R.L.: Aileron Controls for Wind Turbine Applications, NASA TM-86867, August 1984.

5. Snyder, Melvin H. and Staples, David L.: Wind II Users Manual, Wichita State University, July 1982.

TABLE I. - EXPERIMENTAL NO-LOAD EQUILIBRIUM TIP SPEED RATIO FOR THE
38 PERCENT CHORD AILERON-CONTROL ROTOR

Aileron deflection, deg	Equilibrium tip speed ratio equations	Wind speed, mps	Equilibrium, rpm	Equilibrium tip speed ratio
-45	$\lambda = 4.43 - 0.047\ V - 4.63/V$	10	17.13	3.50
		15	25.11	3.42
		20	31.93	3.26
-60	$\lambda = 3.27 - 0.029\ V - 4.49/V$	10	12.40	2.53
		15	18.65	2.54
		20	24.20	2.47
-75	$\lambda = 2.90 - 0.027\ V - 5.49/V$	10	10.21	2.09
		15	15.69	2.14
		20	20.51	2.09
-90	$\lambda = 2.53 - 0.016\ V - 5.41/V$	10	8.95	1.83
		15	14.15	1.93
		20	18.95	1.94
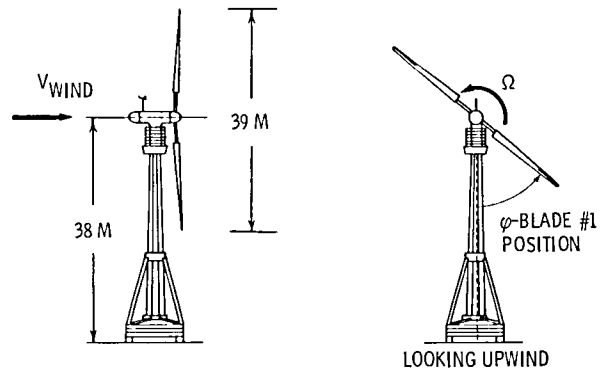
Figure 1 - Configuration of the MOD-O 100 kW wind turbine

NACA 23024 **NACA 64XXX**

STATION, m	BLADE CHORD, m	CONTROL CHORD, m
56	.56	—
1 02	56	—
4 06	1 52	—
7 94	1 52	—
12 22	1 23	—
13 09	1 15	—
13 11	1 15	44
19 20	67	25
19 50	00	

CD-83-13686
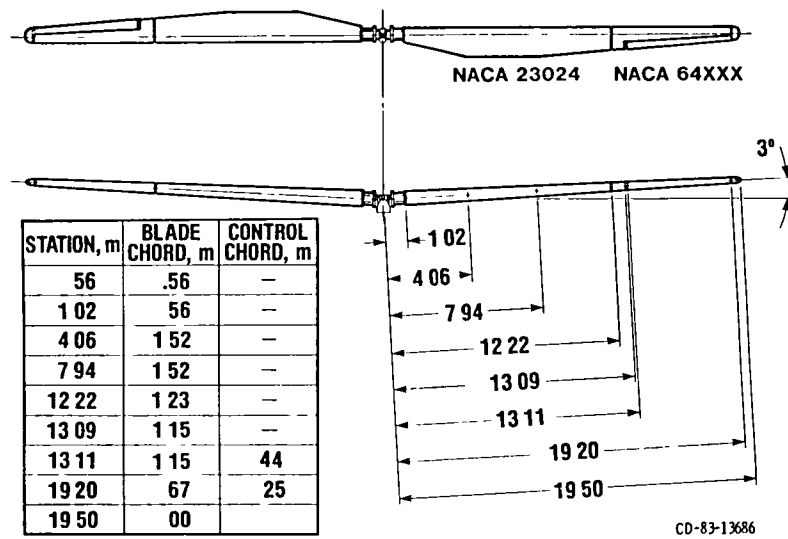
Figure 2 - Teetered, 38 percent chord aileron-control rotor.
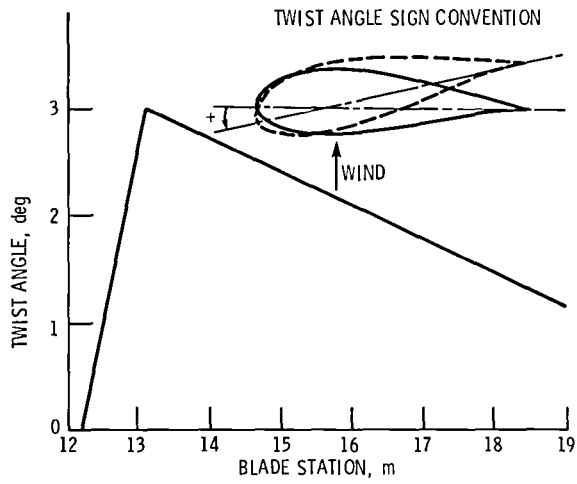
Figure 3 – Twist angle distribution of 38 percent chord aileron-control blade tip
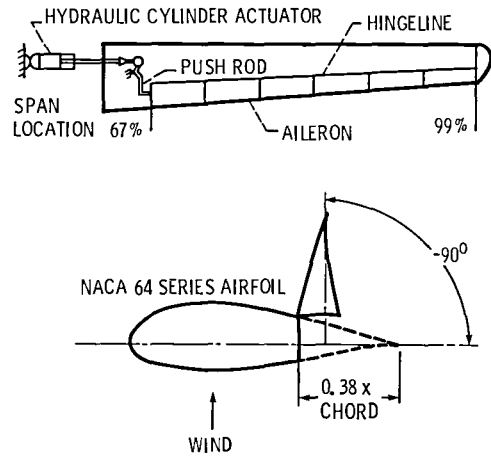
Figure 4 – Planform and cross-section layout of a MOD-O blade tip with a 38 percent chord aileron

OVERSPEED
TEST

NO-LOAD EQ
rpm TEST

PEAK ROTOR SPEED

CONSTANT
DECELERATION

20

ROTOR SPEED, rpm

PEAK
OVERSPEED

0

TIME

INCREASING
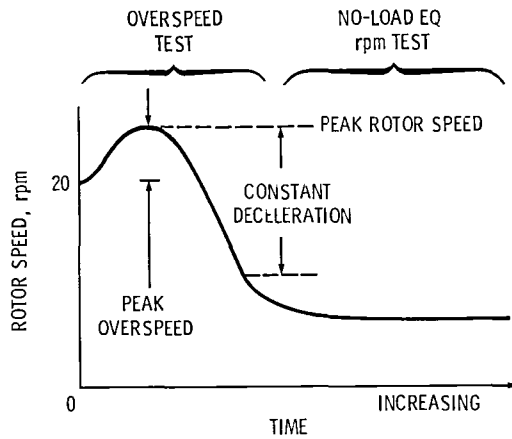
Figure 5 - Aileron-control shutdown tests
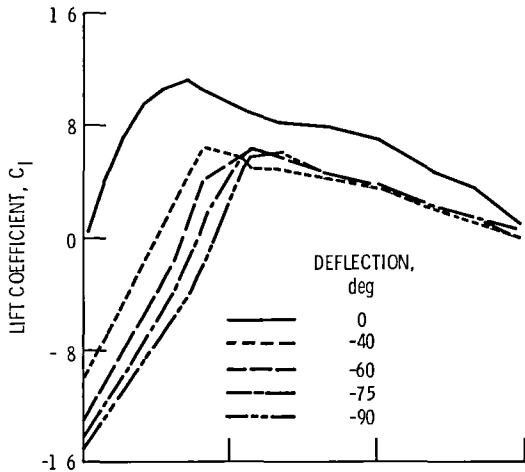
1 6

LIFT COEFFICIENT, C$_l$

8

0

- 8

-1 6

DEFLECTION,
deg
0
-40
-60
-75
-90

(a) Lift coefficient for aileron-control tip   (NACA
64 series airfoil, Reynolds number, 1 5x10^6)

1 6

DRAG COEFFICIENT, C$_d$

1 2

8

4

0

DEFLECTION,
deg
0
-40
-60
-75
-90

(b) Drag coefficient for aileron-control tip   (NACA
64 series airfoil, Reynolds number, 1 5x10^6)

1 6

LIFT COEFFICIENT, Cl

1 2

8

4

0

POST STALL SYNTHESIZED

2-D DATA

30

60

90

(c) Lift coefficient for inboard blade. (NACA
23024 airfoil; Reynolds number, 0.6x10^6.)

2 0

DRAG COEFFICIENT, C$_d$

1 6

1 2

8

4

0

2-D DATA

POST STALL SYNTHESIZED

30

60

90

ANGLE OF ATTACK, deg
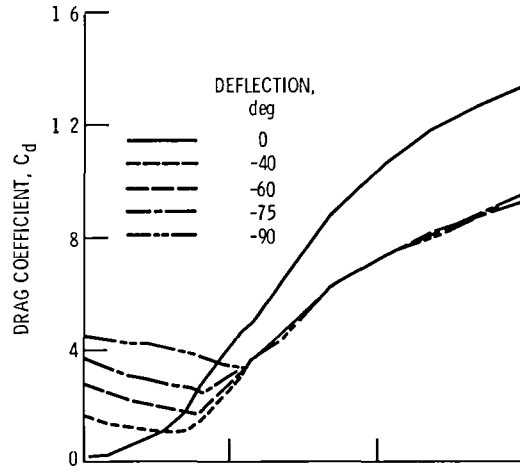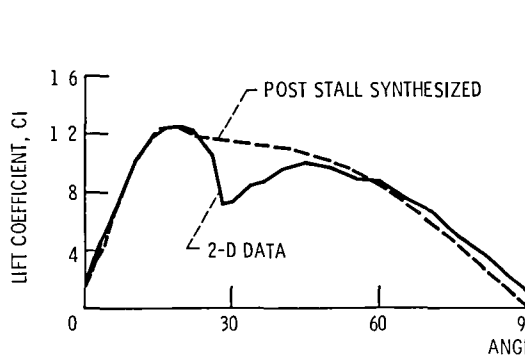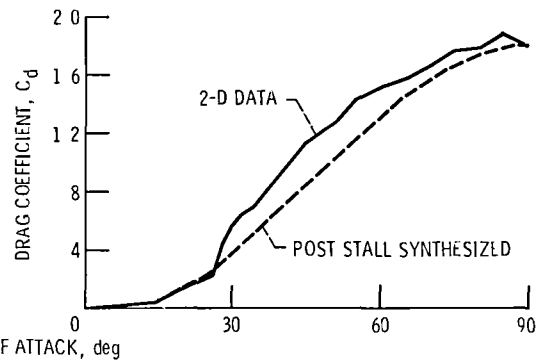
(d) Drag coefficient for inboard blade. (NACA
23024 airfoil; Reynolds number, 0.6x10^6.)

Figure 6 - Aerodynamic data for 38 percent chord aileron-control rotor
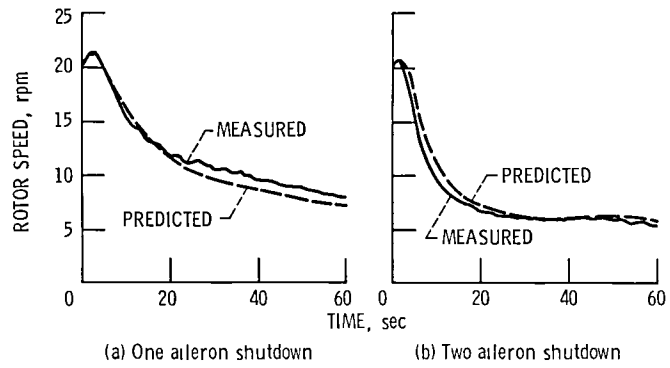
(a) One aileron shutdown   (b) Two aileron shutdown

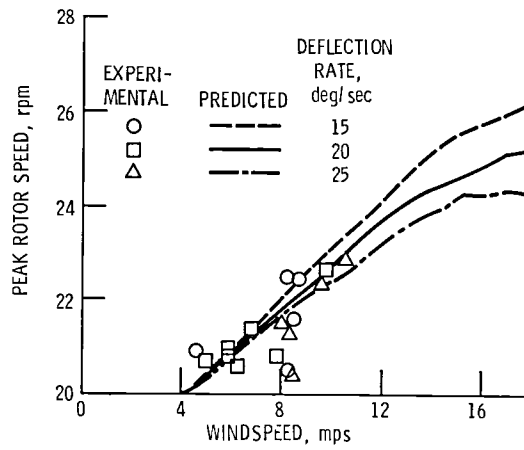Figure 7 - Typical rotor speed time history during loss-of-load shutdown

Figure 8 - Peak rotor speed following loss of generator load (2-aileron shutdown)
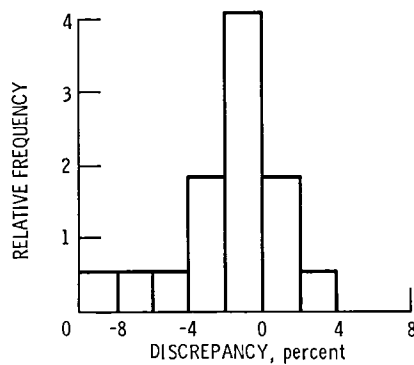

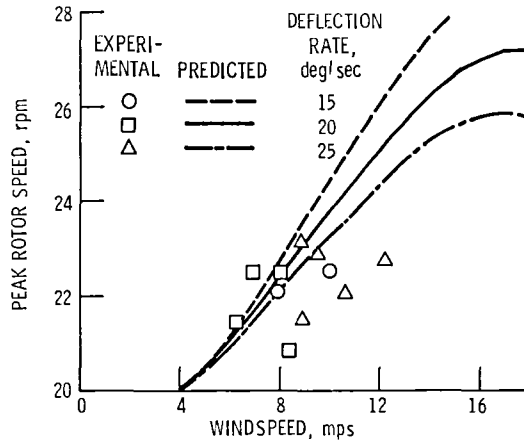Figure 9 - Histogram of discrepancy between experimental and predicted peak rotor speed (2-aileron shutdown)

Figure 10 - Peak rotor speed following loss of
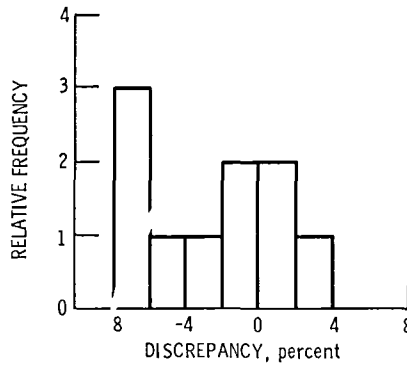generator load (1-aileron shutdown)

Figure 11 - Histogram of discrepancy be-
tween experimental and predicted peak
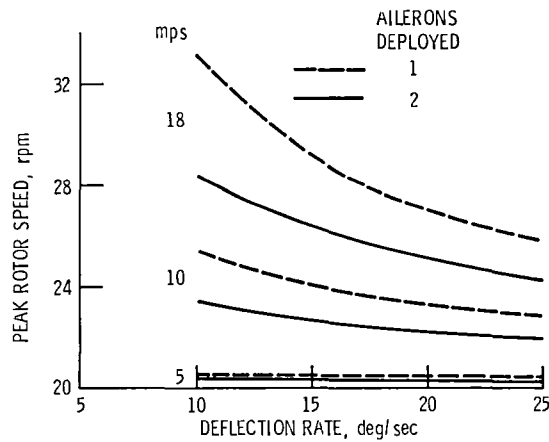rotor speed (1-aileron shutdown)

Figure 12 - Predicted effect of deflection rate on peak
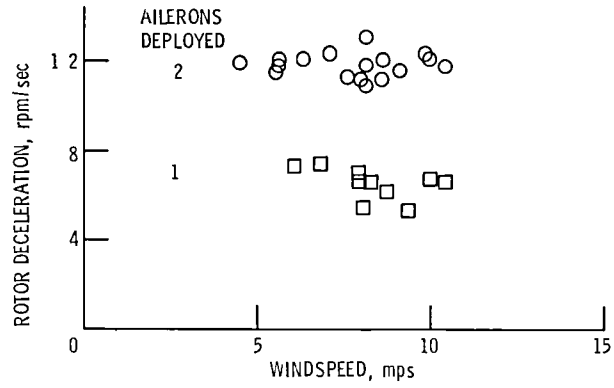rotor speed for various windspeeds

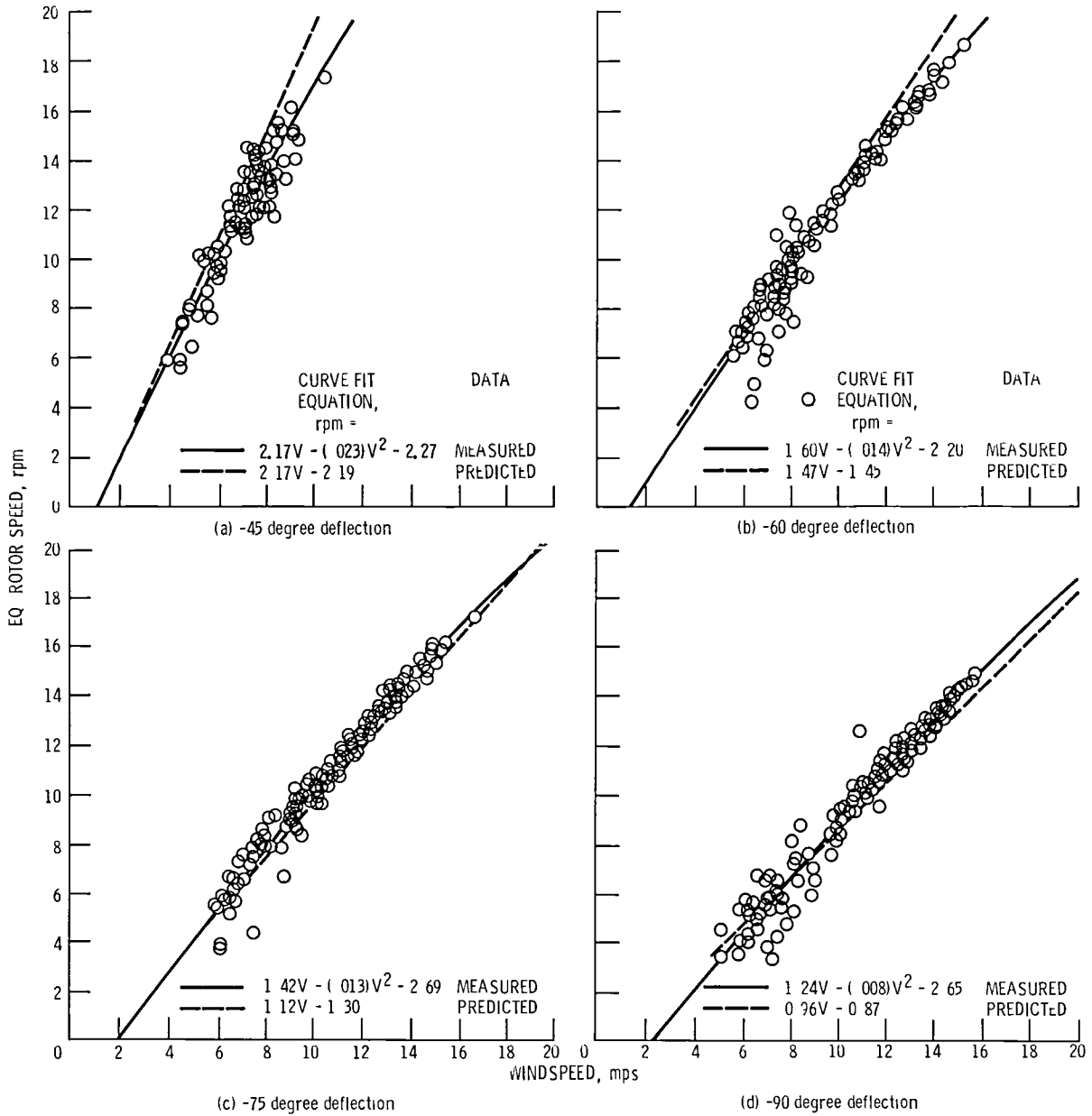Figure 13 - Experimental rotor deceleration just after peak rotor speed

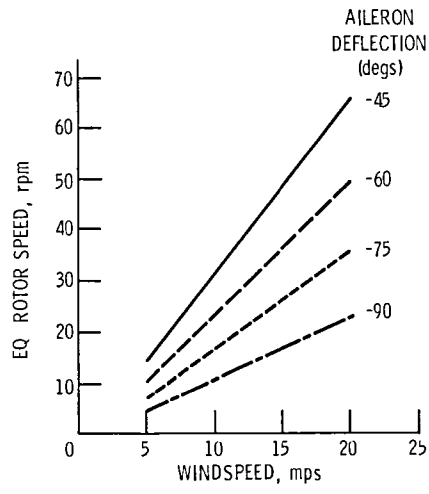Figure 14 - No-load equilibrium rotor speed with 2 ailerons deployed

Figure 15. - Predicted no-load equilibrium
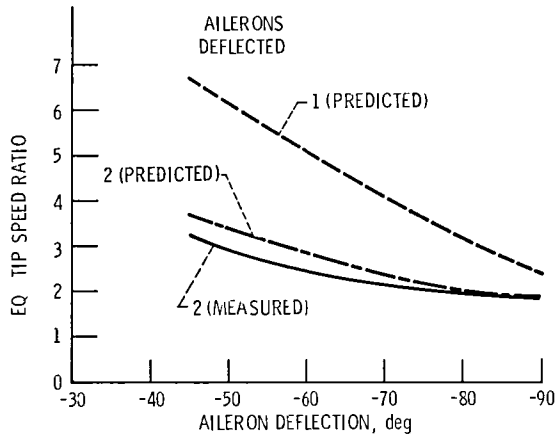rotor speed with 1-aileron deployed.

Figure 16 - Comparison of experimental and predicted
no-load equilibrium tipspeed ratios (windspeed =
20 mps)

1 Report No	2 Government Accession No	3 Recipient's Catalog No
NASA TM-86918		

4 Title and Subtitle	5 Report Date
Shutdown Characteristics of the Mod-0 Wind Turbine with Aileron Controls	
	6 Performing Organization Code
	776-33-41

7 Author(s)	8 Performing Organization Report No
Dean R. Miller and Robert D. Corrigan	E-2410
	10 Work Unit No

9 Performing Organization Name and Address	11 Contract or Grant No
National Aeronautics and Space Administration Lewis Research Center Cleveland, Ohio 44135	
	13 Type of Report and Period Covered

12 Sponsoring Agency Name and Address	Technical Memorandum
U.S. Department of Energy Wind Energy Technology Division Washington, D.C. 20545	14 Sponsoring Agency Code Report No.
	DOE/NASA/20320-61

15 Supplementary Notes

Final report. Prepared under Interagency Agreement DE-AI01-76ET20320. Prepared for Horizontal-Axis Wind Turbine Technology Workshop cosponsored by the U.S. Department of Energy and the NASA Lewis Research Center, Cleveland, Ohio, May 8-10, 1984.

16 Abstract

Horizontal-axis wind turbines utilize partial or full variable blade pitch to regulate rotor speed. The weight and costs of these systems indicated a need for alternate methods of rotor control. Aileron control is an alternative which has potential to meet this need. The NASA Lewis Research Center has been experimentally testing aileron control rotors on the Mod-0 wind turbine to determine their power regulation and shutdown characteristics. This paper presents experimental and analytical shutdown test results for a 38 percent chord aileron-control rotor. These results indicated that the 38 percent chord ailerons provided overspeed protection over the entire Mod-0 operational windspeed range, and had a no-load equilibrium tip speed ratio of 1.9. Thus, the 38 percent chord ailerons had much improved aerodynamic braking capability when compared with the first aileron-control rotor having 20 percent chord ailerons.

17 Key Words (Suggested by Author(s))	18 Distribution Statement
Wind turbine shutdown; Aileron-control rotor; Wind turbine loss-of-load shutdown	Unclassified – unlimited STAR Category 44 DOE Category UC-60

19 Security Classif (of this report)	20 Security Classif (of this page)	21 No of pages	22 Price*
Unclassified	Unclassified		A02

End of Document